



HAL
open science

Theoretical investigation of the platinum substrate influence on BaTiO₃ thin films polarisation

Pierre-Marie Deleuze, Agnes Mahmoud, Bruno Domenichini, Céline Dupont

► **To cite this version:**

Pierre-Marie Deleuze, Agnes Mahmoud, Bruno Domenichini, Céline Dupont. Theoretical investigation of the platinum substrate influence on BaTiO₃ thin films polarisation. *Physical Chemistry Chemical Physics*, 2019, 21, pp.4367-4374. 10.1039/C8CP07022A . hal-03032729

HAL Id: hal-03032729

<https://hal.science/hal-03032729>

Submitted on 1 Dec 2020

HAL is a multi-disciplinary open access archive for the deposit and dissemination of scientific research documents, whether they are published or not. The documents may come from teaching and research institutions in France or abroad, or from public or private research centers.

L'archive ouverte pluridisciplinaire **HAL**, est destinée au dépôt et à la diffusion de documents scientifiques de niveau recherche, publiés ou non, émanant des établissements d'enseignement et de recherche français ou étrangers, des laboratoires publics ou privés.

Cite this: DOI: 10.1039/xxxxxxxxxx

Theoretical investigation of the platinum substrate influence on BaTiO₃ thin films polarisation.

Pierre-Marie Deleuze,^a Agnes Mahmoud,^a Bruno Domenichini,^a and Céline Dupont^{*a}

Received Date
Accepted Date

DOI: 10.1039/xxxxxxxxxx

www.rsc.org/journalname

Density functional theory calculations are performed to study the out-of-plane polarisation in BaTiO₃ (BTO) thin films epitaxially grown on platinum. Prior to any polarisation calculation, the stability of the Pt(001)/BaTiO₃(001) structure is thoroughly discussed. In particular, the nature of the Pt/BTO and BTO/vacuum interfaces is characterised. The growth of BTO is shown to start with a TiO₂ layer while the nature of the surface termination does not broadly modify the stability. Therefore both upper terminations are considered when describing the ferroelectric behaviour in Pt/BTO interfaces. The geometric and electronic effects of the substrate on the polarisation are investigated. To isolate the electronic influence of platinum, the out-of-plane polarisation in Pt/BTO systems is compared to the one in isolated BTO slabs constrained to the same lattice mismatch induced by the epitaxial growth on platinum. The ferroelectric phase is favoured as soon as the thickness is larger than 23 Å, both for isolated and deposited BTO, for the smallest width. The Pt substrate will modify the size of polarisation domains, while an upper BaO layer through the use of asymmetric [TiO₂/BaO] systems, will induce an increase of the polarisation. One could take advantage of this experimentally.

1 Introduction

Efficient use of renewable energies represent one of the main challenges of the last decades. Among them, solar energy can be used to produce hydrogen through water photo electrolysis. To do so, metal oxide could constitute a wide class of suitable materials, however their efficiency is often very poor. Several reasons can be invoked, like the wrong conduction band alignment of usual metal oxide catalysts as well as the decrease of the electron-hole recombination rate¹⁻⁴. While an external bias can be used to align bands properly, the most profitable option is to find an internal solution. From this point of view, the ability of ferroelectric materials to exhibit an intrinsic polarisation and thus a permanent internal electric field is a great opportunity. As a consequence, ferroelectric materials have set off considerable attention in the past years for photocatalytic reactions⁵⁻⁷ or photovoltaic devices⁸⁻¹⁰. Moreover, several studies have showed that the dipolar field can influence charge carrier transport leading to a spatial localisation of the electron and hole half reactions¹¹⁻¹⁴. Hence, it is of primary importance to study the factors influencing the polarisation in order to take advantage of it.

Among possible ferroelectric oxides, BaTiO₃ (BTO) has been extensively studied over the last decades as it stands for an archety-

pal ferroelectric perovskite. At high temperature, it shows a paraelectric cubic structure where Ba²⁺ ions are located at the corners, O²⁻ ions at the center of the faces and a Ti⁴⁺ ion at the body center of the cell. Below the Curie temperature (around 120°C), BTO undergoes a transition to a tetragonal ferroelectric phase which exhibits a spontaneous polarisation along the [001] direction. The cubic phase of BTO(001) has already been experimentally described¹⁵ as well as its tetragonal phase¹⁶⁻¹⁸. Numerous studies¹⁹⁻²⁶ have been devoted to BaTiO₃ involved in capacitors, namely BTO sandwiched between two electrodes. All these studies have allowed the characterisation of different properties of BTO, such like the critical thickness required for polarisation. On the contrary, only few studies have considered BTO thin films on a substrate, while it could be of great interest to take advantage of the surface properties of polarised films. Barbier and coworkers^{1,27} as well as Lu *et al.*²⁸ have experimentally explored the polarisation of BTO thin films deposited on Nb:SrTiO₃ photo anodes. In the meantime, Pancotti *et al.*²⁹ have combined X-Ray Photoelectron Diffraction (XPD) and multiple scattering simulations to characterize the surface rumpling and relaxation of ferroelectric BTO(001) single crystal. Theoretically, very few studies have been dedicated to BTO thin films. Meyerheim *et al.*^{30,31} have considered BaTiO₃ over either Fe, Pt or Pd(001) surfaces, but only in its paraelectric phase. Recently³² the out-of-plane polarisation of BTO has been carefully described for isolated BTO. However, this differs from reality because BTO thin films are rarely used alone

^a Address, Laboratoire Interdisciplinaire Carnot de Bourgogne (ICB), UMR 6303 CNRS, Université de Bourgogne Franche Comté, BP 47870, 21078 Dijon Cedex, France; E-mail: celine.dupont@u-bourgogne.fr

but rather deposited on a conductive substrate such as Pt which offers good conductive properties as well as suitable epitaxy conditions. The substrate can broadly modify structural, electronic and polarisability properties of the overlayer. To take advantage as much as possible of ferroelectricity of BTO, it thus appears essential to thoroughly characterise its properties when grown over a realistic substrate.

Hence, in this paper, we present a detailed description of the nature of the Pt(001)/BTO(001) interface. Then, we report a thorough analysis of the geometric and electronic influence of Pt substrate, as well as the influence of the thickness and the nature of the termination of the overlayers on the BTO polarisation.

2 Computational details

Density Functional Theory (DFT) calculations were performed using the Vienna *ab initio* simulation package VASP code^{33,34}. The calculations were carried out with a plane-wave energy cutoff of 500 eV. The projector augmented wave (PAW) potentials were used to describe the electron-ion interaction^{35,36}, which explicitly included ten valence electrons for Ba ($5s^2 5p^6 6s^2$), six for O ($2s^2 2p^4$), twelve for Ti ($3s^2 3p^6 4s^2 3d^2$) and ten for Pt ($5d^9 6s^1$). The generalised gradient approximation (GGA) was employed with Perdew-Burke-Ernzerhof (PBE)³⁷ exchange correlation functional. As it is well known that DFT has issues to properly describe the strong correlation between *d* electrons, the DFT+U approach was used by including an on-site Coulomb repulsion U-term for the Ti 3d electrons, adopting the Dudarev method³⁸. The effective parameter $U_{eff}=3.5$ eV was applied and allowed to increase the band gap to 2.23 eV, getting closer to the experimental value (3.2 eV)³⁹. This also allows to avoid spurious charge transfer between the substrate and the overlayer; results obtained in this way compare well with previous study.⁴⁰

The convergence threshold on total energy was set to 10^{-6} eV. The structural optimisation was stopped when the forces converged below 0.01 eV/Å. In the following, different periodicities of unit cells have been considered; a $7 \times 7 \times 1$ Monkhorst-Pack⁴¹ *k*-point mesh was used to sample the first Brillouin zone for the smallest periodicity. For larger cells, the grid was adapted accordingly.

Prior to any surface calculation, tetragonal bulk BTO was modeled. The lattice parameters of the stable structure was found to be $a = 4.006$ Å and $c = 4.184$ Å corresponding to a c/a ratio of 1.044. These values are in pretty good agreement with other DFT studies⁴²⁻⁴⁶ where a has been calculated between 3.954 and 4.013 Å for a c/a ratio between 1.006 and 1.045, depending on the level of calculations. This also fits with experiments which have measured $a = 3.991$ Å, $c = 4.036$ Å and thus $c/a = 1.011$ at room temperature.¹⁸ Following the Berry phase method a spontaneous polarisation of $P = 31.7 \mu\text{C.cm}^{-2}$ was calculated. This value stands in the range (from 24.3 to 35.1 $\mu\text{C.cm}^{-2}$) of previously calculated values^{43,45} and it is a bit higher than the experimental value of 27 $\mu\text{C.cm}^{-2}$ ^{47,48}. However this is consistent with the well-known fact that GGA tends to overestimate the tetragonality of BTO and thus its polarisation.

The Pt(001) substrate was modelled by a five layers slab, in which

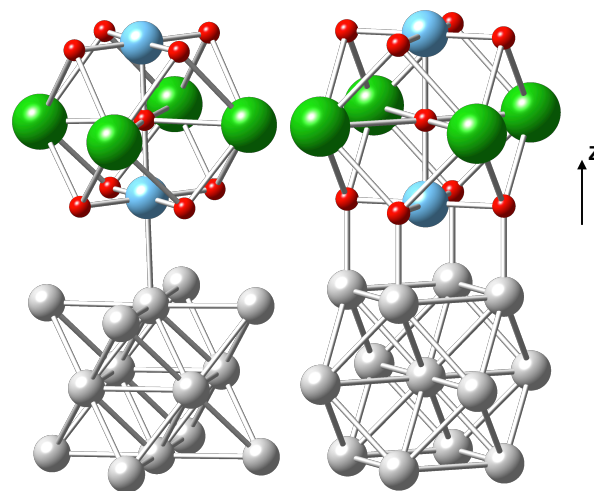


Fig. 1 Side view of the top (left) and hollow (right) adsorption positions of BaTiO₃ on Pt(001) in the case of the Pt/TiO₂ interface. The z axis stands along the [001] direction. For sake of clarity only 3 layers are reported for both the substrate and the overlayer. Pt atoms are reported in gray, Ba in green, Ti in blue and O in red.

the bottom two layers were fixed at their bulk positions. To reproduce as faithfully as possible the experimental strain induced by a platinum substrate on a BTO overlayer, Pt was described with its experimental lattice constant, namely $a_{Pt} = 3.92$ Å, inducing a 2.1% lattice mismatch for epitaxially grown BTO. Influence of thickness was considered through BTO slabs from 7 to 15 layers, while influence of width, through slabs of different periodicities. In each case, all atoms of BTO slabs, either isolated or deposited, were allowed to relax. A 20 Å vacuum was used to separate periodic images along the z direction.

3 Results

3.1 The Pt/BaTiO₃(001) interface

Before studying the polarisation of the BTO thin films, it is mandatory to properly describe the Pt(001) / BaTiO₃(001) interface. Several combinations have to be taken into account. First both terminations of BTO, namely TiO₂ and BaO, have to be considered for each interface: the Pt/BTO one and the BTO/vacuum. At this stage, an additional parameter occurs: the Pt/BTO alignment for the growth of the first layer. In the following "Top" and "Hollow" will refer to the position of the Ti (resp. Ba) atoms of the BTO first layer regarding to the Pt surface, as reported on Figure 1 for the Pt/TiO₂ interface. To analyse these interfaces, we have considered the adhesion energy defined as: $E_{adh} = E_{(Pt/BTO)} - E_{(Pt)} - E_{(BTO)}$. This energy was decomposed into two components through the following equation: $E_{adh} = E_{int} + E_{strain}$. The former is negative and corresponds to the interaction between BTO and Pt, while the latter is positive and corresponds to the strain induced in BTO by the epitaxy. All numerical results are summarised in Table 1.

First of all, Pt/TiO₂ and Pt/BaO interfaces behave quite differently. While hollow and top position can barely be distinguished when growth starts through BaO surface, the hollow site is clearly

on Pt		5 layers Pt			
		TiO ₂		BaO	
upper termination		TiO ₂	BaO	TiO ₂	BaO
E_{strain}		30	32	32	43
Top	E_{adh}	12	17	-15	12
	E_{int}	-19	-15	-47	-32
	$d_{Pt/cat}$	2.79	2.84	3.37	3.35
Hollow	E_{adh}	-31	-30	-17	10
	E_{int}	-62	-62	-50	-33
	$d_{Pt/cat}$	2.19	2.20	3.77	3.78

Table 1 Adhesion energies, E_{adh} (in $\text{meV}\cdot\text{\AA}^{-2}$), interaction energies, E_{int} (in $\text{meV}\cdot\text{\AA}^{-2}$), and distances, $d_{Pt/cat}$ (in \AA), between Pt from the substrate and cation (Ba or Ti) from the deposit, for an overlayer of BTO deposited on a Pt(001) slab. For symmetric overlayers, namely $[\text{TiO}_2/\text{TiO}_2]$ (or $[\text{BaO}/\text{BaO}]$), a BTO thin film of 11 layers is used, while for asymmetric ones, namely $[\text{TiO}_2/\text{BaO}]$ (or $[\text{BaO}/\text{TiO}_2]$), the films present a 10 layers thickness. Top and hollow refer to the position of the first layer cations (Ba or Ti) towards platinum.

favoured when TiO_2 is in contact with platinum. The similarity between top and hollow sites for the Pt/BaO interface is directly related to the weak Pt/Ba interaction, leading to a large distance between the two surfaces. As reported in Table 1, the distance between platinum and baryum is more than 3 \AA : 3.4 and 3.8 \AA for top and hollow sites, respectively. This wide gap between both interfaces neutralises the effects related to different adsorption sites. This is confirmed by the fact that the substrate/layer interaction (E_{int}) is identical for both positions. Hence, when growth starts from the BaO termination, the only difference comes from the upper termination. In fact, the symmetric $[\text{BaO}/\text{BaO}]$ overlayers are slightly unstable ($E_{adh} \approx 15 \text{ meV}/\text{\AA}^2$) while asymmetric $[\text{BaO}/\text{TiO}_2]$ ones present a small stabilisation ($E_{adh} \approx -15 \text{ meV}/\text{\AA}^2$). This disparity can be analysed through the nature (symmetric or asymmetric) of the overlayer, leading to different sensitivities to interlayers relaxations induced by the presence of the substrate only on one side.

On the contrary, for the Pt/ TiO_2 interface, top and hollow positions can be easily distinguished: the hollow adsorption is favoured, while the top one is unstable. This comes mainly from the strain induced over BTO by the substrate. When it grows over platinum, BTO endures a 2.1% geometrical constraint due to the difference of lattice parameter with platinum. This strain leads to an energy cost around $30 \text{ meV}/\text{\AA}^2$ for both $[\text{TiO}_2/\text{TiO}_2]$ and $[\text{TiO}_2/\text{BaO}]$ BaTiO_3 slabs. Hence, even if the Pt/ TiO_2 interface interaction energies are always negative, the stabilisation observed for top position is not large enough to overcome the strain cost. As a consequence, the final adhesion energy is positive leading to an unfavored growth over top positions. These results are consistent with previous studies. In particular Rappe and coworkers²⁶ also found that the Pt/ TiO_2 interface with Ti atoms in hollow sites is the most stable. As shown by Stengel *et al.*²⁰, this is mainly related to the nature of the Pt-O bond. Indeed, when Ti atoms are located on hollow sites, all surrounding oxygens are on top of Pt atoms (see Figure 1), leading to a strong interaction. According to results reported above, in the following we will only focus on the Pt/ TiO_2 interface, with Ti atoms on hollow sites.

3.2 Stability of ferroelectric phases

Up to now only one theoretical study³² has considered the out-of-plane polarisation of BTO not involved in capacitors. This lack of studies, despite numerous potential applications, is certainly due to the strong limitations induced by the modelling of such a system. In fact thin films of ferroelectrics, accumulate charges at their surface. This leads to an electric field (called depolarising field) which tends to counter this accumulation to put the system back to neutral. Hence to keep the out-of-plane polarisation, it is mandatory to use a computational protocol that avoids this depolarisation. Different methods,^{42,49–51} all presenting pros and cons, have already been proposed. In the following we will apply the method firstly introduced by Migoni *et al.*⁵² for a molecular dynamics study of deposited PbTiO_3 thin films and then developed by Shimada⁵¹ for periodic DFT study of free-standing PbTiO_3 thin films. This method consists in dividing the thin films into two domains of opposite polarisation, in order to obtain a simulation cell without any net dipole moment, thus preventing all depolarisation issues. One non negligible advantage of this method is that beyond the calculation trick, this also depicts the reality. In fact the existence of polydomains has already been evidenced experimentally for such ferroelectrics^{53–55}.

In the case of BTO deposited on platinum, the metallic character of the substrate allows a charge accumulation which compensates the surface charge of the ferroelectric¹⁹, and thus simplifies issues relative to depolarisation. However, this accumulation at the bottom interface can not be infinite - this would lead to a divergence of the system -, thus the use of the opposite domains' model^{51,52} is still necessary to create some alternation of charge accumulation and depletion in the top layers of the substrate, leading the remaining of platinum unaffected. Besides, the thickness of platinum substrate required for surface dipole convergence has also been checked. Contrary to what happens in capacitors⁵⁶, five layers of platinum are sufficient for overlayers.

First of all, we have determined the BTO critical thickness required to favour the ferroelectric phase. To do so, symmetric $[\text{TiO}_2/\text{TiO}_2]$ BTO systems from 7 to 15 layers have been considered, either isolated or deposited on Pt substrate. We first discuss only the two unit cells periodicity. To analyse the electronic influence of the substrate on the polarisation, BTO deposited on platinum is compared with isolated BTO already constrained at the Pt lattice parameter, namely 3.92 \AA . The relative stability of ferro- and paraelectric phases is compared for all these cases and reported on Figure 2. According to these results the stability of the ferroelectric phase over the paraelectric one increases as the thickness increases, especially over platinum. Nevertheless, the presence of platinum has no influence on the critical thickness that stabilises polarised systems: in both cases symmetric ferroelectric systems are stable for slabs of 11 or more layers, namely 23 \AA .

Critical thickness has also been determined for the four and six unit cells periodicity. While it remains unchanged for isolated BTO (see Figure 2), in presence of platinum ferroelectric phase

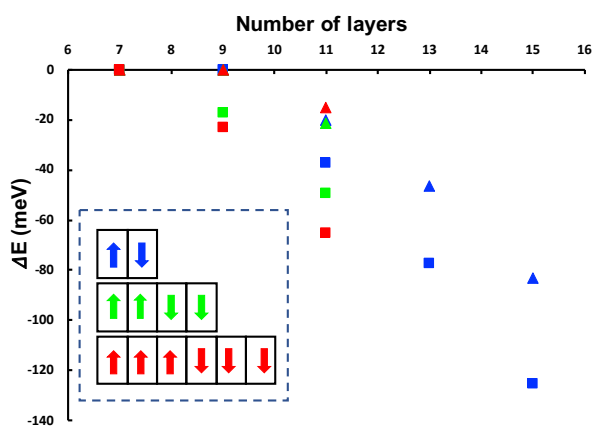


Fig. 2 Relative stability between ferroelectric and paraelectric phases: $\Delta E = (E_{ferro} - E_{para})/(N/2)$ in meV, as a function of the number of layers and of the number of lateral unit cells (N). Triangles correspond to isolated strained BTO, squares to BTO deposited on Pt. Periodicities of two ($N=2$), four ($N=4$) and six ($N=6$) unit cells are reported in blue, green and red, respectively. For sake of clarity, these three periodicities are sketched in the insert.

is stabilised from 9 layers, demonstrating a different behaviour between free-standing and deposited BTO. This result confirms the role of boundary conditions, already evidenced both theoretically⁵² and experimentally⁵⁷, on the critical thickness. The influence of lateral periodicity has been carefully analysed for the 11 layers films, with and without platinum. For the later case, our findings are fully consistent with previous results of Dionot *et al.*³²: systems with width of 2 or 4 unit cells are the most stable (ΔE around 20 meV), while those with 6 unit cells of periodicity are not favoured with $\Delta E = -15$ meV. This behaviour is substantially modified by the presence of platinum. In fact, the larger stabilisation of the ferroelectric phase over the paraelectric already observed for the 2 unit cells system, is still present, but is even larger as the periodicity increases. Hence for BTO deposited on Pt, the six unit cells systems (sketched in red in the insert of Figure 2) is clearly favoured.

3.3 Polarisation patterns

Starting from the 11 layers thin films, the local polarisation has been analysed in details. To do so, the polarisation of each unit cell centered on an oxygen atom of a BaO layer (delimited with lines on Figure 3) has been calculated with the formula developed by Vanderbilt⁵⁸ and already used by Shimada⁵¹:

$$\mathbf{P} = \frac{e}{\Omega_c} \sum_j \omega_j \mathbf{Z}_j^* \mathbf{u}_j,$$

where e and Ω_c refer to the electron charge and the volume of the unit cell, respectively. The index j of the sum covers all atoms in the unit cell, with ω_j and \mathbf{u}_j , the weight of atom j in the unit cell and its atomic displacement vector from the ideal lattice position, respectively. Finally, \mathbf{Z}_j^* is the Born effective charge tensor of atom j in the cubic bulk of BaTiO₃.

The local polarisations are reported for each unit cell on

Figure 3 for both isolated strained and deposited BTO. The left side corresponds to the P_{up} polarisation, with displacements of Ti atoms outwards, while the right side corresponds to the P_{down} with displacements of Ti atoms inwards. Reported values correspond only to the contribution along the Z axis. In fact for the two unit cells periodicity, lateral contributions are null. We first focus on isolated strained BTO. While the increase of the thickness favours the ferroelectric phase towards the paraelectric one, there is no crucial change in polarisation patterns. A low polarisation (between 5 and 12 $\mu\text{C}\cdot\text{cm}^{-2}$) is always observed at the surface, while polarisation of central unit cells increases as the thickness increases, to get closer to the strained bulk polarisation. In fact when a 2.1% compressive strain is applied to the BTO bulk, its polarisation increases from 31.7 to 37.1 $\mu\text{C}\cdot\text{cm}^{-2}$. This corresponds to a gain of almost 20% of polarisation, in agreement with previous results: Junquera and Ghosez¹⁹ have observed a 29% increase for BTO involved in capacitors with the same kind of constraint. Qualitatively, this behaviour fully agrees with the previous study of Dionot *et al.*³², for a 3.8% constraint. The electronic influence of platinum on the polarisation is now considered for the two unit cells periodicity. First of all, despite the use of symmetric initial configurations, optimised ferroelectric BTO over Pt, presents clear dissymmetries of local polarisation (see Figure 3). If this loss of symmetry has to be analysed, it is worth mentioning that it has no consequence such as the appearance of a depolarising field as mentioned above. Indeed, the presence of a metallic substrate allows accumulation of charges which compensate the ferroelectric surface charge density¹⁹. Three parts can thus be distinguished in the overlayers. First of all the upper part, namely the surface unit cells close to vacuum, presents a polarisation similar to the one observed without Pt. Absolute values between 5 and 15 $\mu\text{C}\cdot\text{cm}^{-2}$ are calculated with opposite polarisation for neighbouring cells. For central unit cells, we also observed a behaviour similar to the one of isolated BTO. The local polarisation increases in comparison to the surface values. One can mention that in presence of Pt, polarisation is slightly higher and thus closer to the bulk value. Finally, contrary to other parts of the slab, a strong difference of behaviour occurs at the Pt/BTO interface. The symmetry is broken and neighbouring cells now present a local polarisation with identical orientation, even if the order of magnitude completely differs. This phenomenon can be explained through the bonding of interfacial atoms which can strongly modify the local ferroelectricity, as already evidenced for KNbO₃ capacitors by Tsymal and coworkers²³. According to this study, the bonds created between the substrate and the perovskite impose some movement restrictions for atoms at the boundaries, inducing a local polarisation at the interface even for the paraelectric capacitors. In agreement with these results, we have analysed the displacements of the first layer atoms in the paraelectric phase for our system: the Ti atoms of the first layer are pushed 0.06 Å towards the O atoms in the presence of platinum. This phenomenon is maintained in the ferroelectric phase increasing the P_{down} polarisation and decreasing the P_{up} one, leading to neighbouring cells with polarisation in the same direction. To conclude the bonding of the ferroelectric BTO

over the substrate induces some disruptions on the polarisation in the first deposited layers, and thus will modify the global polarisation: in presence of platinum, the global P_{up} is lowered, while P_{down} is increased. Another important conclusion concerns the dependency of the global polarisation behaviour with the slab thickness. In fact, in both BTO and Pt/BTO cases, as soon as the ferroelectric state becomes stable, the distribution of polarisation along the layers is identical whatever the total size of the slab.

The influence of lateral periodicity is now discussed for the 11 layers thickness. Results for the three considered periodicities, namely 2, 4 and 6 unit cells, are reported on Fig 4. From this graphic, two main conclusions can be drawn. First of all, whatever the periodicity, the platinum has always the same influence on the polarisation. In the three cases we observe the same patterns as previously described for the two cells periodicity, namely a large asymmetry at the Pt/BTO interface, then a polarisation close to the bulk one in the middle cells, finally an opposite polarisation for the neighbouring upper cells. Secondly, contrary to the smallest width, higher periodicities (like 4 and 6 unit cells) allow the appearance of closure domains similar to the ones already observed by Shimada *et al.* for PbTiO_3 ⁵¹. Again, except at the Pt/BTO interface, the presence of the substrate does not have a large influence on the patterns, for a given periodicity. However, the main difference will come from the observed periodicity. As reported on Figure 2, only the 2 or 4 unit cells periodicities are observed for isolated BTO, while in presence of platinum, larger periodicities are favoured, allowing larger domains. As reported on Fig 4, the increase of lateral periodicity leads also to an increase of local polarisation. Hence in presence of platinum, larger domains with higher polarisation are obtained.

3.4 Influence of upper termination

As mentioned above, as soon as the growth starts from TiO_2 interface with Ti in hollow site, the top termination has no influence on the stability. Hence, one can imagine that the film can be terminated either by a BaO or a TiO_2 layer, depending on experimental conditions. It is thus important to study if the modification of the termination has some influence on the intensity of the polarisation. The $[\text{TiO}_2/\text{BaO}]$ slab either isolated or deposited on Pt is thus compared to the reference $[\text{TiO}_2/\text{TiO}_2]$ slab. To allow a thorough comparison, the isolated strained $[\text{BaO}/\text{BaO}]$ slab is also considered. In the case of BaO termination, the local polarisation is calculated in a unit cell centered on a Ti atom from a TiO_2 plan. For the $[\text{TiO}_2/\text{BaO}]$ systems, the asymmetry of the slab prevents the decomposition of the slab in an integer number of unit cells. As we primary focus on the polarisation at the vacuum / slab interfaces, for the asymmetric systems we start the decomposition from the top BaO surface and we do not calculate the local polarisation of the last layer, as reported on Figure 5. As a consequence, the local polarisation is calculated for unit cells centered on Ti atoms as in the case of $[\text{BaO}/\text{BaO}]$ systems.

As for symmetric slabs, the isolated strained systems are first considered. In Figure 6, the local polarisation for the P_{up} and

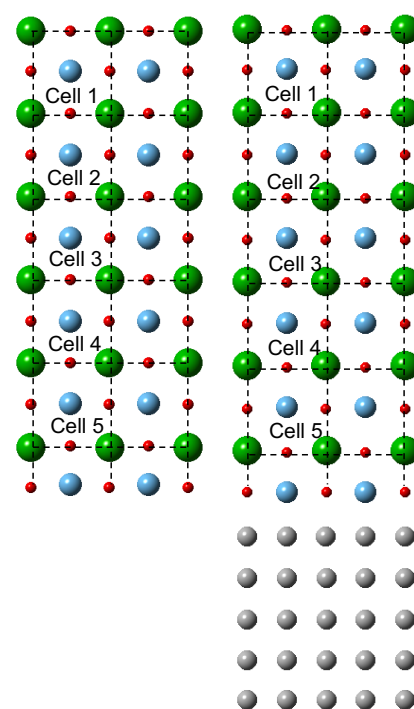


Fig. 5 Paraelectric 12 layer asymmetric $[\text{BaO}/\text{TiO}_2]$ slab either isolated and strained on the left or deposited on platinum on the right. Ba atoms are represented in green, Ti in blue, O in red and Pt in gray. The delimitation as well as the numbering of the cells used for the discussion are also reported.

the P_{down} sides is reported for the first four surface cells (Cells 1 to 4 in Figure 5) of the 11 layers $[\text{TiO}_2/\text{TiO}_2]$ and $[\text{BaO}/\text{BaO}]$ slabs and for the 12 layers $[\text{BaO}/\text{TiO}_2]$. The polarisation of the symmetric $[\text{BaO}/\text{BaO}]$ slab is clearly the highest. This is directly related to the chemical nature of termination. In fact, in the case of BaO terminated slabs, the unit cells recover the original nature of bulk BTO unit cells. The natural movement of Ti atoms is thus favoured, allowing a better amplitude of displacements. The increase of polarisation is especially true at the surface of the P_{down} side and in the center part of the slab. For $[\text{BaO}/\text{BaO}]$ system, the polarisation of the strained bulk is almost reached for cell 3: $P_{up}(\text{Cell 3}) = |P_{down}(\text{Cell 3})| = 32 \mu\text{C}\cdot\text{cm}^{-2}$ ($P_{strained}(\text{bulk}) = 37 \mu\text{C}\cdot\text{cm}^{-2}$). These results clearly show that the $[\text{BaO}/\text{BaO}]$ system has a higher polarisation than the $[\text{TiO}_2/\text{TiO}_2]$ ones. This interesting behaviour is partially kept for asymmetric systems. In fact, as observed on Figure 6, the $[\text{BaO}/\text{TiO}_2]$ system presents an intermediate polarisation between $[\text{TiO}_2/\text{TiO}_2]$ and $[\text{BaO}/\text{BaO}]$. Again, the polarisation of middle cells is increased compared to symmetric TiO_2 systems, as well as the surface polarisation of the P_{down} side.

Finally, the local polarisation of $[\text{BaO}/\text{TiO}_2]$ is now evaluated when it is deposited on Pt. Results are reported on Figure 7. According to this graph, the presence of platinum slightly increases again the value of local polarisation, as found for the $[\text{TiO}_2/\text{TiO}_2]$ system. Hence, using appropriate experimental con-

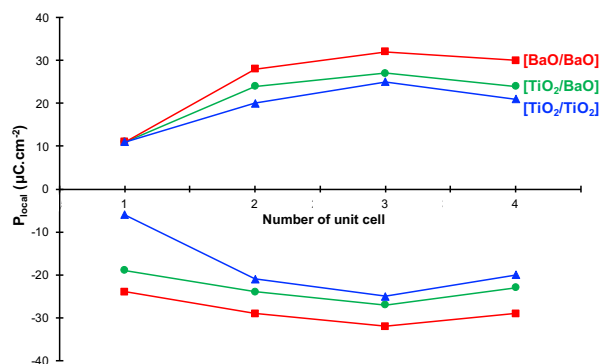


Fig. 6 Evolution of local polarisation (in $\mu\text{C}\cdot\text{cm}^{-2}$) in the symmetric slabs of 11 layers with either two TiO_2 terminations (blue curves with triangles) or two BaO terminations (red curves with squares) and in asymmetric $[\text{TiO}_2/\text{BaO}]$ slabs of 12 layers (green curves with circles). Only values for the four first cells starting from the BaO surface in the case of asymmetric slabs are reported. Positive values refer to the P_{up} side, negative to the P_{down} one.

ditions that lead to an upper BaO termination should allow a higher polarisation and thus modify the properties of the material.

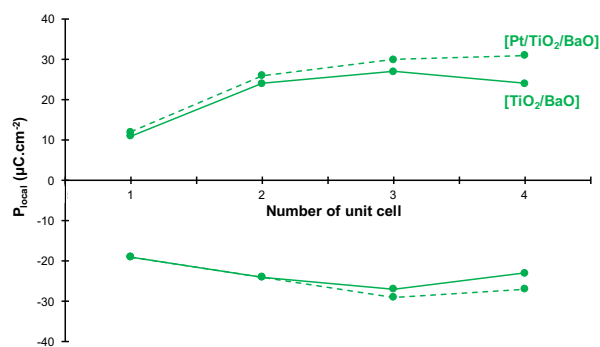


Fig. 7 Evolution of local polarisation (in $\mu\text{C}\cdot\text{cm}^{-2}$) in asymmetric TiO_2/BaO slabs of 12 layers either isolated (plain green curve) or deposited on Pt (dotted green curve) Only values for the four first cells starting from the BaO interface with vacuum are reported. Positive values refer to the P_{up} side, negative to the P_{down} one

4 Conclusions

In summary, we have performed a thorough analysis of the ferroelectric behaviour of $\text{BaTiO}_3(001)$ slabs epitaxially grown on $\text{Pt}(001)$. The paraelectric BTO was firstly considered to determine the nature of the Pt/BTO interface. We thus showed that the growth always starts with the TiO_2 termination with titanium atoms in hollow positions, and oxygen atoms on top of platinum. Under the 2.1% compressive strain induced by the lattice mismatch between the substrate and the overlayer, ferroelectric slabs of BTO are stabilised over paraelectric ones for thicknesses larger than 23 \AA (11 layers). Beyond this thickness, all symmetric $[\text{TiO}_2/\text{TiO}_2]$ slabs present the same evolution of polarisation: local polarisation at the surface is lower than the one calculated inside the slab, which tends to the strained bulk polarisation. The presence of a platinum substrate induces several modifica-

tions on the BTO overlayers. On an energetic point of view, platinum has two consequences. First of all, it increases the stability of ferroelectric slabs over paraelectric ones, and lowers the thickness for stabilising the ferroelectric phase. In presence of platinum, ferroelectric phase is observed from 9 layers for domains of width of two unit cells or more. Secondly, the presence of a substrate modifies the size of the domains. While for isolated BTO slabs, the small two or four unit cells periodicities are favoured over larger ones, in presence of platinum, larger domains will be observed. Concerning the polarisation, at a given periodicity, both deposited and isolated BTO slabs present a similar qualitative behaviour. From a quantitative point of view, three differences have to be mentioned: the stability of ferroelectric slabs over paraelectric ones is increased in the presence of platinum. Secondly, the local polarisation is modified at the Pt/BTO interface because of Pt-O bonding. Thirdly, the local polarisation of the central unit cells is increased in the presence of platinum. Finally an important change due to the presence of platinum, is the kind of observed domains. As larger cells are favoured for overlayers, larger domains with clearer closure walls will be observed.

Finally the influence of the upper termination on the polarisation was also analysed through the study of asymmetric $[\text{TiO}_2/\text{BaO}]$ slabs: the presence of an upper BaO termination induces an increase of the local polarisation of the middle cells, but also of the surface polarisation of the P_{down} side.

Acknowledgements

Calculations were performed using HPC resources from DNUM CCUB (Centre de Calcul de l'Université de Bourgogne). The authors also thank the ANR for financial support through project ANR-15-CE05-PHOTO-POT.

Notes and references

- 1 M. Rioult, S. Datta, D. Stanesco, S. Stanesco, R. Belkhou, F. Maccherozzi, H. Magnan and A. Barbier, *Appl. Phys. Lett.*, 2015, **107**, 103901.
- 2 S. Park, C. W. Lee, M.-G. Kang, S. Kim, H. J. Kim, J. E. Kwon, S. Y. Park, C.-Y. Kang, K. S. Hong and K. T. Nam, *Phys. Chem. Chem. Phys.*, 2014, **16**, 10408–10413.
- 3 W. Ji, K. Yao, Y. F. Lim, Y. C. Liang and A. Suwardi, *Appl. Phys. Lett.*, 2013, **103**, 062901.
- 4 Y. Inoue, K. Sato and H. Miyama, *J. Phys.*, 1986, **90**, 2809–2810.
- 5 D. Tiwari and S. Dunn, *J. Mater. Sci.*, 2009, **44**, 5063–5079.
- 6 L. Li, P. A. Salvador and G. S. Rohrer, *Nanoscale*, 2014, **6**, 24–42.
- 7 A. Kakekhani, S. Ismail-Beigi and E. I. Altman, *Surf. Sci.*, 2016, **650**, 302–316.
- 8 M. Qin, K. Yao and Y. C. Liang, *Appl. Phys. Lett.*, 2008, **93**, 122904.
- 9 I. Grinberg, D. V. West, M. Torres, G. Gou, D. M. Stein, L. Wu, G. Chen, E. M. Gallo, A. R. Akbashev, P. K. Davies, J. E. Spanier and A. M. Rappe, *Nature*, 2013, **503**, 509–512.
- 10 Y. Yuan, Z. Xiao, B. Yang and J. Huang, *J. Mater. Chem. A*, 2014, **2**, 6027–6041.

- 11 J. L. Giocondi and G. S. Rohrer, *Chem. Mater.*, 2001, **13**, 241–242.
- 12 J. L. Giocondi and G. S. Rohrer, *J. Phys. Chem. B*, 2001, **105**, 8275–8277.
- 13 N. V. Burbure, P. A. Salvador and G. S. Rohrer, *J. Am. Ceram. Soc.*, 2006, **89**, 2943–2945.
- 14 N. V. Burbure, P. A. Salvador and G. S. Rohrer, *Chem. Mater.*, 2010, **22**, 5831–5837.
- 15 J. W. Edwards, R. Speiser and H. L. Johnston, *J. Am. Chem. Soc.*, 1951, **73**, 2934–2935.
- 16 B. C. Frazer, H. R. Danner and R. Pepinsky, *Phys. Rev.*, 1955, **100**, 745–746.
- 17 J. Harada, T. Pedersen and Z. Barnea, *Acta Crystallogr. Sect. A*, 1970, **26**, 336–344.
- 18 G. H. Kwei, A. C. Lawson, S. J. Billinge and S. W. Cheong, *J. Phys. Chem.*, 1993, **97**, 2368–2377.
- 19 J. Junquera and P. Ghosez, *Nature*, 2003, **422**, 506.
- 20 M. Stengel, D. Vanderbilt and N. A. Spaldin, *Nat. Mater.*, 2009, **8**, 392.
- 21 M. Stengel, D. Vanderbilt and N. A. Spaldin, *Phys. Rev. B*, 2009, **80**, 224110.
- 22 Y. Umeno, B. Meyer, C. Elsässer and P. Gumbsch, *Phys. Rev. B*, 2006, **74**, 060101(R).
- 23 C. Duan, R. Sabirianov, W. Mei, S. Jaswal and E. Tsymbal, *Nano Lett.*, 2006, **6**, 483.
- 24 P. Aguado-Puente and J. Junquera, *Phys. Rev. Lett.*, 2008, **100**, 177601.
- 25 Y. Umeno, J. Albina, B. Meyer and C. Elsässer, *Phys. Rev. B*, 2009, **80**, 205122.
- 26 N. Sai, A. Kolpak and A. Rappe, *Phys. Rev. B*, 2005, **72**, 020101(R).
- 27 S. Datta, M. Rioult, D. Stanescu, H. Magnan and A. Barbier, *Thin Solid Films*, 2016, **607**, 7–13.
- 28 H. A. Lu, L. A. Wills and B. W. Wessels, *Appl. Phys. Lett.*, 1994, **64**, 2973–2975.
- 29 A. Pancotti, J. Wang, P. Chen, L. Tortech, C. M. Teodorescu, E. Frantzeskakis and N. Barrett, *Phys. Rev. B*, 2013, **87**, 184116.
- 30 H. L. Meyerheim, F. Klimenta, A. Ernst, K. Mohseni, S. Ostanin, M. Fechner, S. Parihar, I. V. Maznichenko, I. Mertig and J. Kirschner, *Phys. Rev. Lett.*, 2011, **106**, 087203.
- 31 H. L. Meyerheim, A. Ernst, K. Mohseni, I. V. Maznichenko, J. Henk, S. Ostanin, N. Jedrecy, F. Klimenta, J. Zegehnagen, C. Schlueter, I. Mertig and J. Kirschner, *Phys. Rev. Lett.*, 2013, **111**, 105501.
- 32 J. Dionot, G. Geneste, C. Mathieu and N. Barrett, *Phys. Rev. B*, 2014, **90**, 014107.
- 33 G. Kresse and J. Furthmüller, *Phys. Rev. B*, 1996, **54**, 11169–11186.
- 34 G. Kresse and J. Furthmüller, *Comput. Mater. Sci.*, 1996, **6**, 15–50.
- 35 P. E. Blöchl, *Phys. Rev. B*, 1994, **50**, 17953–17979.
- 36 K. G. and D. Joubert, *Phys. Rev. B*, 1999, **59**, 1758–1775.
- 37 J. P. Perdew, K. Burke and M. Ernzerhof, *Phys. Rev. Lett.*, 1996, **77**, 3865–3868.
- 38 S. Dudarev, G. Botton, S. Savrasov, C. Humphreys and S. A.P., *Phys. Rev. B*, 1998, **57**, 1505–1509.
- 39 K. Suzuki and K. Kijima, *Jpn. J. Appl. Phys.*, 2005, **44**, 2081.
- 40 M. Stengel, P. Aguado-Puente, N. A. Spaldin and J. Junquera, *Phys. Rev. B*, 2011, **83**, 235112.
- 41 J. D. Pack and H. J. Monkhorst, *Phys. Rev. B*, 1977, **16**, 1748–1749.
- 42 M. Fechner, S. Ostanin and I. Mertig, *Phys. Rev. B*, 2008, **77**, 094112.
- 43 N. Iles, K. Driss Khodja, A. Kellou and P. Aubert, *Comput. Mater. Sci.*, 2014, **87**, 123–128.
- 44 D. I. Bilc, R. Orlando, R. Shaltaf, G. M. Rignanese, J. Íñiguez and P. Ghosez, *Phys. Rev. B*, 2008, **77**, 165107.
- 45 E. S. Goh, L. H. Ong, T. L. Yoon and K. H. Chew, *Comput. Mater. Sci.*, 2016, **117**, 306–314.
- 46 R. A. Evarestov and A. V. Bandura, *J. Comput. Chem.*, 2012, **33**, 1123–1130.
- 47 W. J. Merz, *Phys. Rev.*, 1953, **91**, 513–517.
- 48 H. H. Wieder, *Phys. Rev.*, 1955, **99**, 1161–1165.
- 49 Y. Mi, G. Geneste, J. Rault, C. Mathieu, A. Pancotti and N. Barrett, *J. Phys.: Condens. Matter*, 2012, **24**, 275901.
- 50 B. Meyer and D. Vanderbilt, *Phys. Rev. B*, 2001, **63**, 205426.
- 51 T. Shimada, S. Tomoda and T. Kitamura, *Phys. Rev. B*, 2010, **81**, 144116.
- 52 M. Sepliarsky, M. G. Stachiotti and R. L. Migoni, *Phys. Rev. Lett.*, 2006, **96**, 137603.
- 53 S. K. Streiffer, J. A. Eastman, D. D. Fong, C. Thompson, A. Munkholm, M. V. R. Murty, O. Auciello, G. R. Bai and G. B. Stephenson, *Phys. Rev. Lett.*, 2002, **89**, 067601.
- 54 N. Spaldin, *Science*, 2004, **304**, 1606.
- 55 D. Fong, G. B. Stephenson, S. Streiffer, J. Eastman, O. Auciello, P. Fuoss and C. Thompson, *Science*, 2004, **304**, 1650.
- 56 A. M. Kolpak, N. Sai and A. M. Rappe, *Phys. Rev. B*, 2006, **74**, 054112.
- 57 P. Gao, Z. Zhang, M. Li, R. Ishikawa, B. Feng, H. J. Liu, Y. L. Huang, N. Shibata, X. Ma, S. Chen, J. Zhang, K. Liu, E. G. Wang, D. Yu, L. Liao, Y. H. Chu and Y. Ikuhara, *Nat. Com.*, 2017, **8**, 15549.
- 58 W. Zhong, R. D. King-Smith and D. Vanderbilt, *Phys. Rev. Lett.*, 1994, **72**, 3618.

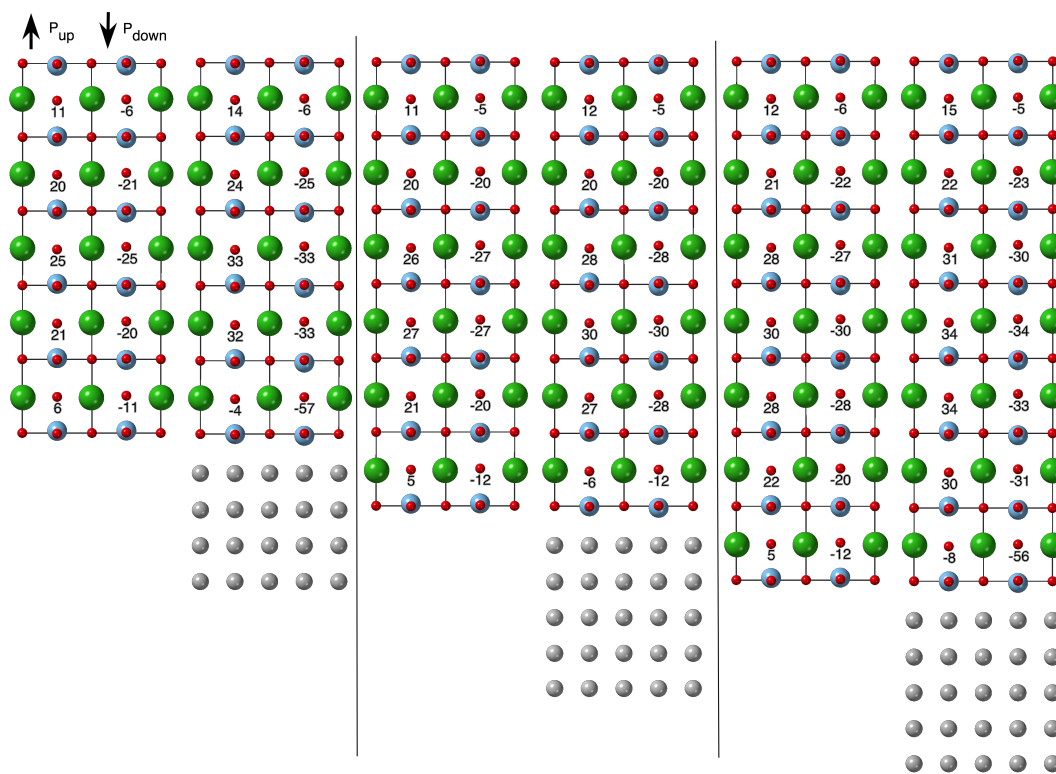


Fig. 3 Evolution of local polarisation as a function of BTO thickness for the two unit cells lateral periodicity. From left to right, slabs of 11, 13 and 15 layers are considered. In each case, both isolated strained BTO and BTO deposited on Pt substrate are reported. Ba atoms are represented in green, Ti in blue, O in red and Pt in gray. Values of local polarisation in the out-of-plane direction is reported for each unit cell in $\mu\text{C}\cdot\text{cm}^{-2}$.

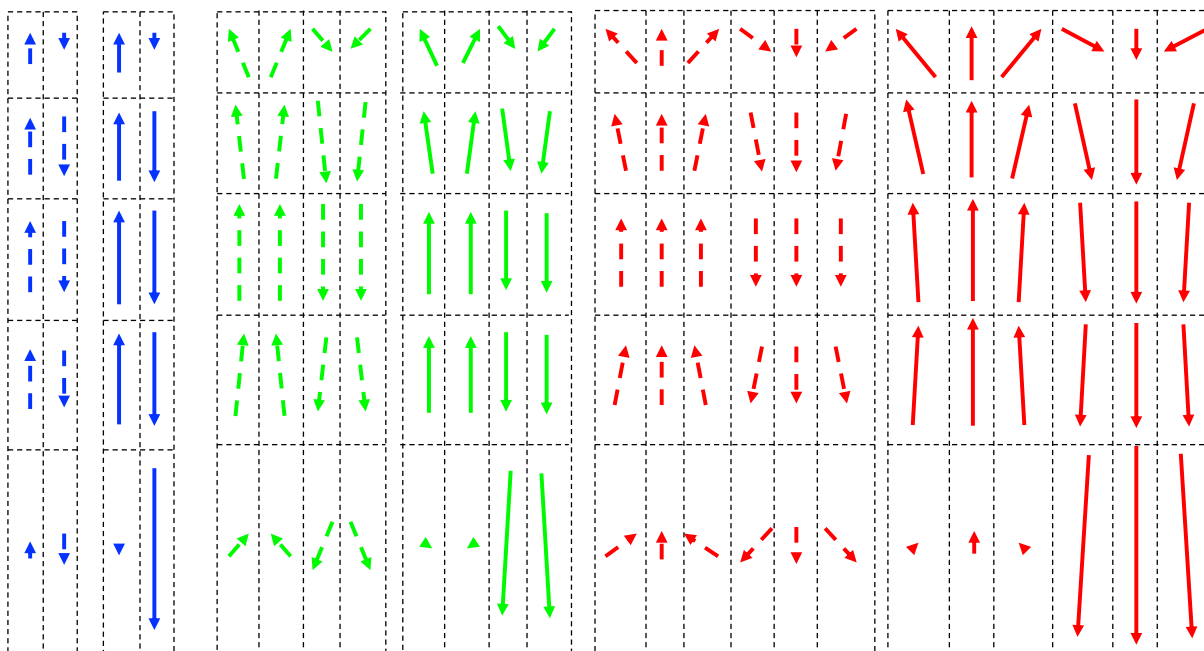


Fig. 4 Vectorial representation of local polarisation for two (in blue), four (in green) and six (in red) unit cells periodicities, for the 11 layers slab. Both isolated BTO (dotted arrows) and BTO deposited on Pt (plain lines arrows) are reported. Black dotted cells are guidelines. They represent, without respect of the scale, the unit cells centered on an oxygen atom of a BaO layer, used for the calculation of local polarisation. Cells in contact with Pt are the ones at the bottom of the pictures, while the interface with vacuum is at the top.